

Elements Synthesized as a Result of Irradiation with Braking Rays γ And By Electrons of A Maximum Energy of 10MeV the Mixture of Helium Gas and Deuterium under High Pressure - Process Theory

Wiśniewski R^{1*}, Mishinsky G.V², Wilczyńska-Kitowska T³ and Semin W.A²

¹Institute of Biotechnology of the Agricultural and Food Industry, Warsaw University of Technology, Faculty of Physics (1952–2000, currently prof. em.), ZFCS NCBJ Otwock-Świerk (2000-2014), Poland.

²Laboratory for Nuclear Reaction, Joint Institute for Nuclear Research, Dubna, Russian Federation.

³ZFCS NCNR (1968-2014), IBSFI Warsaw, Poland

*Correspondence:

Wiśniewski Roland, Institute of Agricultural and Food Biotechnology. Rakowiecka 36, 02-532 Warsaw, Poland, E-mail: roland.wisniewski@gmail.com.

Received: 14 May 2022; Accepted: 20 Jun 2022; Published: 25 Jun 2022

Citation: Wiśniewski R, Mishinsky G.V, Wilczyńska-Kitowska T, et al. Elements Synthesized as a Result of Irradiation with Braking Rays γ And By Electrons of A Maximum Energy of 10MeV the Mixture of Helium Gas and Deuterium under High Pressure - Process Theory. Nano Tech Appl. 2022; 5(1): 1-10.

ABSTRACT

The paper describes an experiment of irradiation - with braking quanta γ and electrons with $E_{max} = 10\text{MeV}$ and with an intensity of about $20\ \mu\text{A}$ - of a mixture of He-D₂ gases (33/67%) at an initial pressure of about 1800 bar in sufficient long time to observe expected results. The preceding experiment with gamma irradiation of the research system did not lead to noticeable changes. After the experiment with electrons, an analysis of objects exposed and available with the help of a scanning microscope with an X-ray microprobe was carried out. Particularly interesting was the radical change in the composition of the near-surface layer (2-3 μm) of elements made of beryllium bronze and pure copper, as well as founded small free particles in the form of small foils of a majority composition – carbon, oxygen and magnesium. The experiment is a continuation of our research related to the phenomenon of low-energy nuclear transmutations (not to be confused with the so-called cold fusion), a new field of knowledge, independent of the phenomena described by its fundamental part - nuclear physics.

Keywords

γ -, e- irradiation, He-D₂ mixture, Transmutation of elements, High pressure.

Introduction

The aim of this paper is to present the results of the first experiment of the electron beam exposure on dense gases (in this case a mixture of He-D₂). The effects of gamma-ray irradiation of dense gases previously observed by the authors are described in [1-5]. "Impossible" radiation less and low-energy nuclear reactions (LENR) were discovered at the end of the last century, in the years 1989-1992 [6], i.e. cold fusion reactions and low-energy transmutation reactions. It turned out that nuclear reactions with the transformation of some chemical elements into other chemical elements can occur in weakly excited condensed matter with a low, only $< 10\ \text{eV/atom}$, excitation energy in the reaction area. This phenomenon received its name: low-energy transmutation of

chemical elements (hereinafter transmutation). The methodologies of transmutation experiments are extremely diverse and fundamentally different from between the methods of nuclear physics. It is recommended to read the papers on this research by G. V. Mishinsky items [6-13] in particular his recent work [7].

The discovered transmutation reactions have been carried out in many laboratories in many processes such as: in glowing gas discharges; in the industrial process of electron melting of zirconium ingots in a vacuum furnace; during explosions on metal objects irradiated by strong pulses of electrons; during explosions in liquid dielectric media of metal films, through which a strong pulse of electric current passed; after exposure of current pulses in the alloy of lead and copper; during the flow of electric current in water-mineral media; during the purifying ultrasonic treatment of aqueous saline solutions; during irradiation of dense gases with gamma braking quanta; in developing biological structures and

in many others. The results of transmutation experiments, despite their diversity, are qualitatively similar to each other.

G.V. Mishinsky proposed the explanation of the mechanism of formation of new nuclei in the case of irradiation of pure helium under high pressure by very strong magnetic interactions in the appropriate concentration of orthohelium [8]. Orthohelium is obtained because of ionization by gamma radiation of parahelium atoms with subsequent recombination of their ions. The orthohelium atom, in which electron spins and, accordingly, their magnetic moments are parallel to each other, has magnetic fields: ~ 400 T at the center of the atom, in the region of the nucleus and ~ 70 T at its diameter $\sim 1.75 \cdot 10^{-10}$ m. Therefore, orthohelium atoms are attracted to each other, combine and create multinuclear molecules, in which transmutation reactions take place. Proposed by R. Wiśniewski an analogous experiment with a mixture of helium and deuterium (in an approximate composition of 33/67 at. %), in which no significant changes were observed, makes the theory of G.V. Mishinsky more probable. Taking into account the results from He (also from H_2 and D_2 [4]) and from Xe [5], we can talk about new - with the participation of low-energy nuclear reactions - macro, micro and nano technologies.

Portable high-pressure apparatus

For the research, a modified apparatus was used - previously used for tests with pure dense gases of helium, deuterium and hydrogen - shown in Fig. 1. The last charge of it was to filling it with helium to half the predicted value of the maximum pressure, then complementing it with spectrally pure deuterium. This meant an increased number of deuterium atoms over the number of helium atoms in the experiment, which guaranteed some "isolation" of the helium atoms relative to each other.

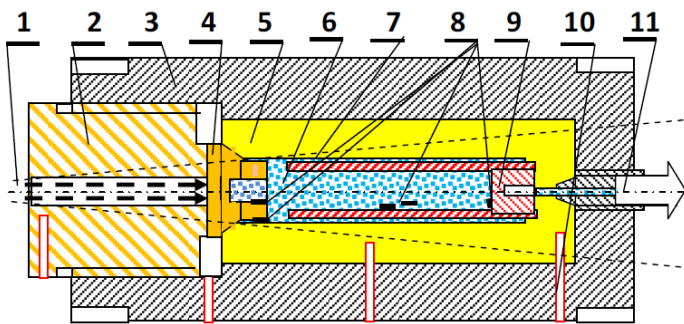


Figure 1: Schematic drawing of the high-pressure chamber: 1 – electron flux (previously γ quanta), 2 – closing screw (CuBe2), 3 – strengthening the body of the high-pressure chamber (mat. SS), 4 – "window – plug" (CuBe2, cones $58^\circ/60^\circ$), 5 – high-pressure chamber (CuBe2), 6 – helium mixture – high-pressure deuterium, 7 – bipartite sleeve, (pure Cu or CuBe2), 8 – expected reaction product, 9 – plug of bipartite sleeve, 10 – temperature measurement channels, 11 – symbolically: high pressure valve, pressure sensor and gas inlet-outlet system, $<$ an angle of 85° of the dissipated energy.

Irradiation with quanta γ with a maximum energy of 10MeV of a dense mixture of He- D_2 gases.

Irradiation with γ quanta of a dense mixture of He- D_2 gases was aimed at confirming the theory of phenomena occurring in pure He. The presence of deuterium was found to prevent the formation of helium boson complexes (see [7,8]). Orthohelium atoms collide with deuterium molecules and deuterium atoms, and transform into parahelium atoms, which do not have a magnetic field.

The pressure before and after irradiation turned out to be, with high accuracy, the same (see Figure. 2). Gamma quanta after multiple different collisions with particles of dense He- D_2 gas are completely absorbed. The horizontal section presents the thermal equilibrium of the system: absorbed energy = gas energy discharged to the environment, at elevated temperature. The pressure was measured using a strain gauge manometer with a conversion of $1.0 \mu\text{Strain} = 3.0$ bar. The calibration of the system was carried out using the high-pressure standard, namely, "dead weight- simple piston - pressure tester".

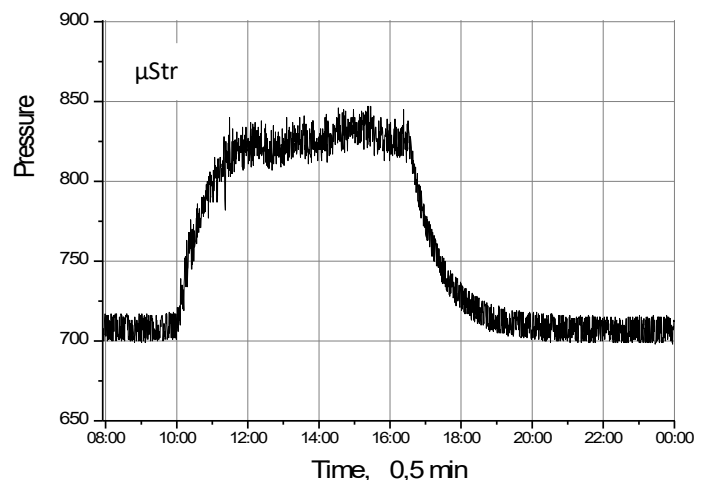


Figure 2: Dependence of pressure changes on the exposure time of a dense mixture of He- D_2 . The irradiation was carried out on - 06.02.2019. Under the direction of G. V. Mishinsky (see photo) Start 9:55:30, end 16:32:30 ($3.4 \cdot 10^4$ s), electron current intensity 20-22 μA . The initial pressure was $(710 - 175) \mu\text{Strain} \times 3.0 = 1605$ bar = 161 MPa, the pressure increase 375 bar = 38M Pa (3.0 - pressure scale converter). Maximum temperature 97°C , has been calculated supposing isochoric process.

Irradiation of the gas mixture He- D_2 with high-energy electrons with an average energy of 10MeV

As planned at the beginning of our study, gamma-ray irradiation was the beginning of the study. Subsequently, it was planned to use high-energy electrons (and other elementary particles). The first applications of electron irradiation (in addition, with basic quanta γ) have already taken place in our research. This applies to the so-called Annavit and the so-called "Dubna oscillations" [1]. Below is shown the result of electron irradiation of a mixture of He and D_2 in a chamber in which gamma irradiation was previously used (without observing typical effects). In the case of electron irradiation, a high increase in pressure and temperature

was observed in a short time. For safety reasons, the accelerator power has been turned off. Unusual behavior of the system was observed. The gas pressure dropped to the ambient pressure. The simplest interpretation is the appearance of a leak in the system exactly when the exposure process was turned off. However, this seems unlikely. Answers to these doubts can only be provided by a thorough analysis of the tightness of the system. Figure. 3 presents the observed course of the experiment.

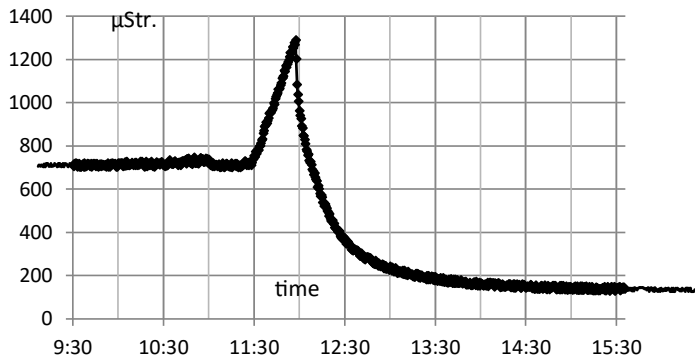
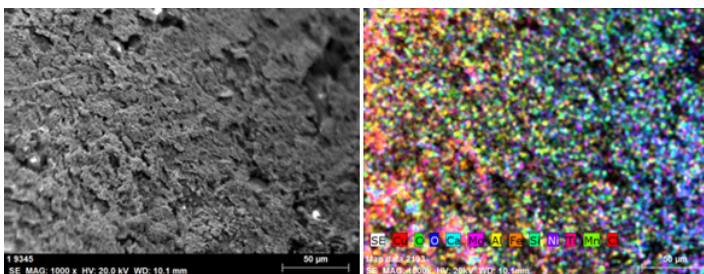


Figure 3: The effect of electron irradiation of a dense mixture of He-D₂. Electron energy 10 MeV; exposure time - 29 min (only), electron current intensity 16 µA. Tests were performed on 27.03.2019. Start 11:29:30, End 11:58:30, Observed pressure increase 3 (1280 – 710 µStr) = 1710 bar, maximum pressure: 3.0 x (1280 – 175 µStr) = 1105x3 = 3315 bar. Temperature at maximum pressure is supposing to be close to those as in the first experiment.

Analysis of the composition of synthesized free objects, the internal surface of a two-part shielding sleeve, sleeve cork and window-cork using scanning electron microscope with X-ray microprobe EDS

Synthesized free objects Figure 1(8)

As mentioned in the introduction, in cases of irradiation with ray's γ the dense gases, macroscopic objects with original compositions were obtained. In the current experiment, three - rather microscopic - flat objects with a thickness of the order of nanometers, a dimension of a characteristic frontal surface of about one mm and a typical gray-black color were inventoried. (see Figure 4). The composition of one such object is shown in Table 1 and in Figure 5.



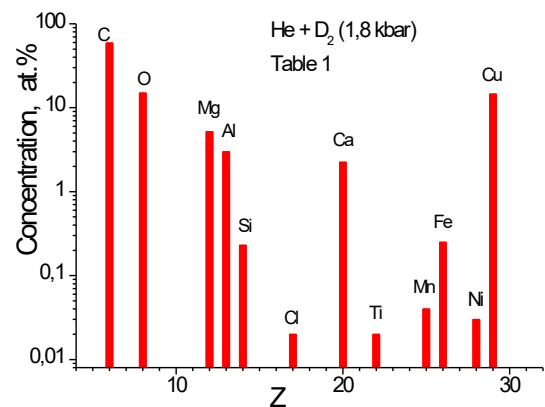
Figures 4: A SEM photo of a selected fragment of a free object and map of its main components suggesting their certain heterogeneity.

Table 1 - Figure 5: Composition of one of the free objects shown in Figure 1(8).

Element Series	unn. [wt.%]	C norm. [wt.%]	C Atom. [at.%]	C Error (3 σ) [wt.%]
Copper K-	99.71	42.10	14.61	8.29
Carbon K-	76.58	32.34	59.36	33.73
Oxygen K-	25.75	10.87	14.99	12.26
Calcium K-	9.70	4.10	2.25	1.07
Magnesium K-	13.58	5.73	5.20	2.65
Aluminium K-	8.69	3.67	3.00	1.58
Iron K-	1.49	0.63	0.25	0.27
Silicon K-	0.70	0.30	0.23	0.27
Nickel K-	0.20	0.09	0.03	0.13
Titanium K-	0.12	0.05	0.02	0.13
Manganese K-	0.22	0.09	0.04	0.14
Chlorine K-	0.07	0.03	0.02	0.12

Figure 5: The cork of the bipartite sleeve Figure 1(7)

In Figure 6, one can say, a random place on the forehead of the cork is shown, considering it typical. This is a natural view, informing about the rather strange structure of the surface. The cork before irradiation had a smooth frontal surface, polished with diamond powder. The surface change currently observed resembles experiencing Pd, irradiated in dense deuterium by gamma quanta and by small dose of electrons. On the right side, visualizations of this surface are shown by recording the main component C. Below are the results of the analysis of the X-ray micro probe system (Table 2 - Figure 7).



Figures 6: Photo SEM of a strongly altered surface of a cork bushing selected as a typical place of the frontal surface of the object (dimension 0.052mm²) and distribution visualization of its main component after the irradiation process – C.

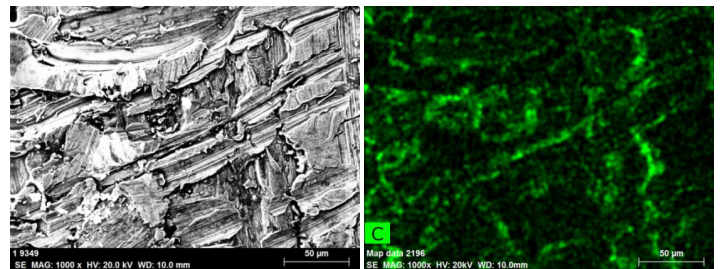


Table 2 - Figure 7: Composition of the front surface of the cork of the bipartite bushing.

Element Series un.	C norm. [wt.%]	C Atom. [wt.%]	C Error (3σ) [at.%]	C Error (3σ) [wt.%]
Copper K-	66.13	72.61	35.46	5.38
Carbon K-	19.64	21.57	55.72	7.48
Oxygen K-	2.95	3.24	6.29	1.32
Silicon K-	0.24	0.27	0.29	0.11
Aluminium K-	1.27	1.39	1.60	0.27
Iron K-	0.48	0.53	0.29	0.12
Sulfur K-	0.13	0.14	0.14	0.09
Chlorine K-	0.11	0.12	0.11	0.09
Calcium K-	0.11	0.13	0.10	0.09
Total:	91.08	100.00	100.00	

Element Series un.	C norm. [wt.%]	C Atom. [wt.%]	C Error (3σ) [at.%]	C Error (3σ) [wt.%]
Copper K-	77.32	83.16	48.97	6.29
Carbon K-	14.01	15.07	46.95	5.84
Oxygen K-	1.58	1.70	3.99	0.85
Silicon K-	0.06	0.07	0.09	0.09
Total:	92.98	100.00	100.00	

Data on changes in the composition and condition of the cork-window surface Figure 1(4).

As already mentioned in the introduction, a place of intense changes was noticed on the cork-window, perhaps related to the fact that the system leaked.

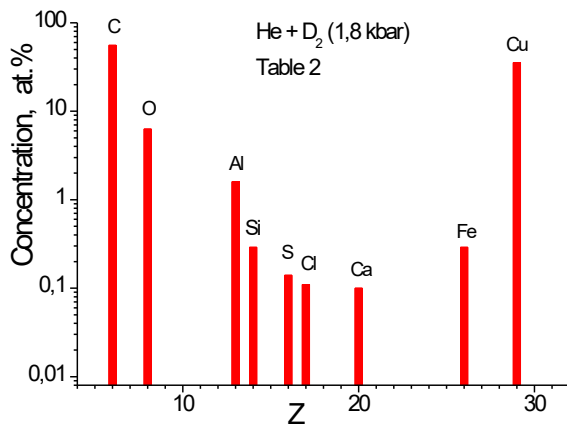
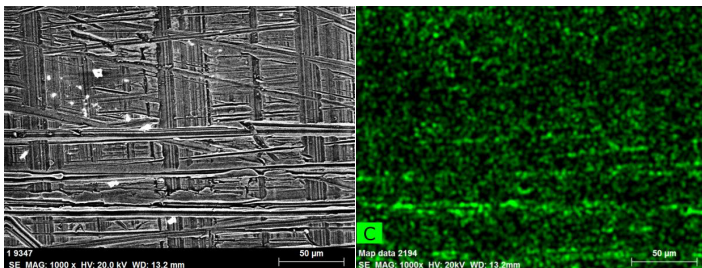


Figure 7:

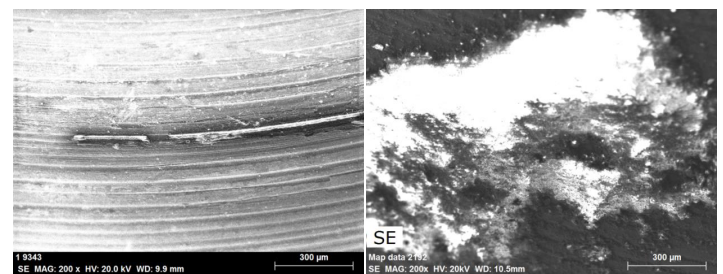
Two-part inner sleeve Figure 1(9)

In Figure 8, the photograph of the inner surface of the split bushing with the area around the center is shown. The observed irregularities are smaller but also surprising. Figure 8b illustrates the distribution of the main element - C. The cited data on the composition of the inner near-surface layer (3μm) in Table. 3 can be considered as a presentation of the entire inner surface of the bushing. Specifically, the data refer to the inside of a random half in its – approximately - central position.

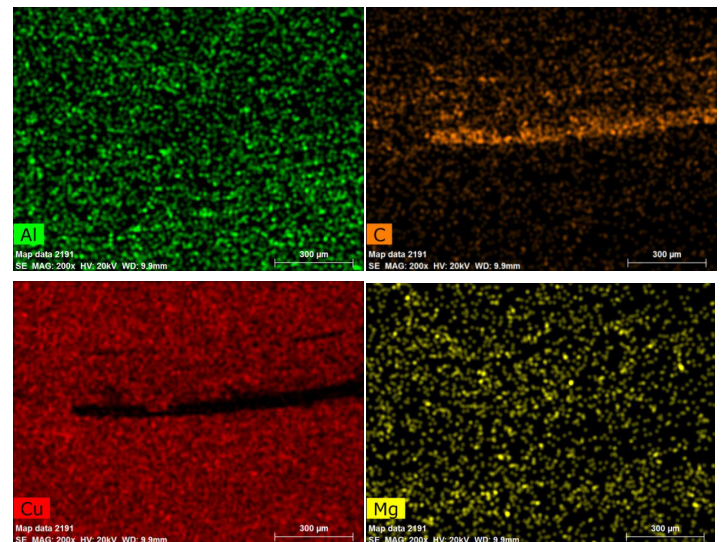


Figures 8: Photograph SEM of the inner surface of the split bushing with the area of the center. The observed inequalities are smaller but also surprising. On the right, the map of the main appeared component C is shown.

Table 3: Chemical composition of the bushing in the middle area of the inner surface of the bushing.



Figures 9: Photograph SEM of a clearly altered place and "growths" on the side surface of the cork-window.



Figures 10: Photographs of near-surface distributions of basic new elements in cork-windows.

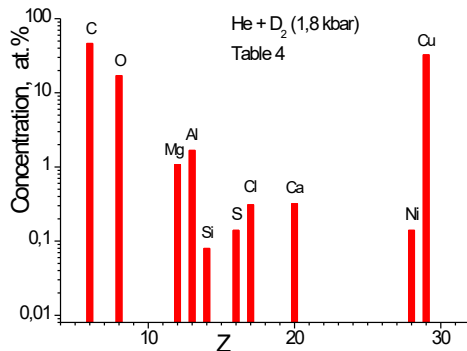
Table 4 - Figure 11 and Table 5 - Figure 12: Composition of new elements in two different places of cork-window, place strongly changed and "growths".

Element Series un. C norm. C Atom. C Error (3σ)
 [wt.%] [wt.%] [at.%] [wt.%]

Copper K-	70.68	68.71	32.59	5.78
Aluminium K-	1.55	1.50	1.68	0.32
Calcium K-	0.43	0.42	0.32	0.13
Chlorine K-	0.38	0.37	0.31	0.13
Oxygen K-	9.35	9.09	17.13	3.89
Magnesium K-	0.90	0.87	1.08	0.25
Carbon K-	19.07	18.54	46.52	8.21
Silicon K-	0.08	0.08	0.08	0.09
Sulfur K-	0.16	0.15	0.14	0.10
Nickel K-	0.28	0.27	0.14	0.12

Total: 102.87 100.00 100.00

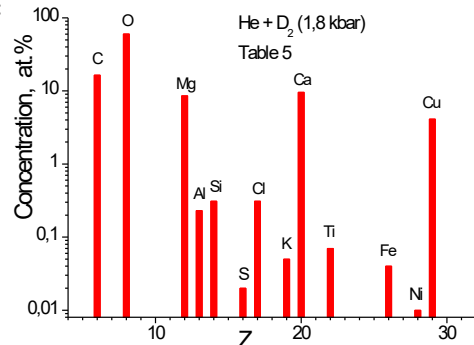
Figure 11:



Element Series un. C norm. C Atom. C Error (3σ)
 [wt.%] [wt.%] [at.%] [wt.%]

Carbon K-	10.32	9.62	16.42	4.77
Oxygen K-	50.43	47.00	60.24	17.95
Magnesium K-	10.93	10.18	8.59	1.88
Aluminium K-	0.32	0.30	0.23	0.13
Silicon K-	0.45	0.42	0.31	0.14
Sulfur K-	0.03	0.03	0.02	0.08
Chlorine K-	0.57	0.53	0.31	0.14
Calcium K-	20.11	18.74	9.59	1.85
Nickel K-	0.03	0.03	0.01	0.09
Copper K-	13.72	12.78	4.13	1.22
Titanium K-	0.18	0.17	0.07	0.10
Potassium K-	0.11	0.10	0.05	0.09
Iron K-	0.10	0.10	0.04	0.10

Figure 12:



Theory of observed phenomena

Analysis of experiments on the transmutation of chemical elements and their results showed that they occur in strong, more than 30 T, magnetic fields. It turned out that atomic and nuclear matter in strong and ultrastrong magnetic fields are transformed into a new state of matter: into a spin nuclide electron condensate. A characteristic feature of such a condensate is that pairwise electrons and pairwise protons and neutrons (fermions with spin equal to $s = 1/2 \hbar$) are in a bound state, in a state of orthobosons in it, when the total spin of each pair is equal to one, $S = 1\hbar$.

Magnetic fields begin to emerge in ionized, liquid media and gaseous media of high pressure because of the passage of unidirectional flows of free electrons with a density of more than 10^{21} cm^{-3} through them [7]. Those magnetic fields owe their origin to the magnetic moments of the electrons μ_e , which are parallel to each other in a unidirectional flow. The magnetic moments of electrons, which move in one direction, are directed, due to the property of helicity, in one direction, in the direction of their momenta. Thus, a directionally moving ensemble of electrons generates a seed magnetic field $B_{\mu 0}$ in a condensed matter, which averaged direction coincides with the direction of electron motion.

Due to its nature, the magnetic field $B_{\mu 0}$, created by the sum of magnetic moments of electrons, is spatially inhomogeneous and anisotropic. Therefore, free electrons, which move in a changing field $\partial B_{\mu 0} / \partial t$ and which have a field-antiparallel orientation of the magnetic moments $B_{\mu 0} \uparrow \downarrow \mu_e$, will change the direction of the magnetic moments μ_e . Thus, the number of free electrons in a state with magnetic moments parallel to the field increases, up to the moment when most electrons would pass into this state. Consequently, the seed magnetic field increases up to saturation B_{μ} . Accordingly, the spins of these electrons will also become parallel. Spin plasma is formed.

Since the electron spins are parallel, then, in addition to the magnetic field, the electrons generate an exchange self-consistent field with a negative potential. Electrons with parallel spins are attracted to each other due to the exchange interaction. The repulsion of free electrons is compensated at densities of $\sim 10^{21} \text{ cm}^{-3}$ by their attraction to positively charged ions, because Debye radius – the distance over which the action of the electric field of a separate charge in a quasi-neutral medium extends, has the size of an atom $\sim 10^{-8} \text{ cm}$.

Electrons with parallel spins in a negative potential, in order to comply with the Pauli principle, are forced to pair into orthobosons with a spin $S = 1\hbar$. This pairing is carried out because electrons in a magnetic field obtain new, oscillatory quantum numbers n_b [11]. An orthobosonic pair of electrons is a toroidal, ring current of radius R_z , which rotates around a counter flow of positive ions that move at a speed V_i (Figure 12a). The orthoboson has external and internal strong magnetic fields B , and a strong electric field. External magnetic fields connect orthobosons into electronic orthoboson “solenoids” - “capsules” (Figure 12b). “Capsules” can have a different number of orthobosons.

Consequently, if electrons move unidirectionally and they have a density $\geq 10^{21} \text{ cm}^{-3}$ in local regions of weakly excited liquid and gaseous media, pairing of electrons into orthobosons will be carried out there automatically.

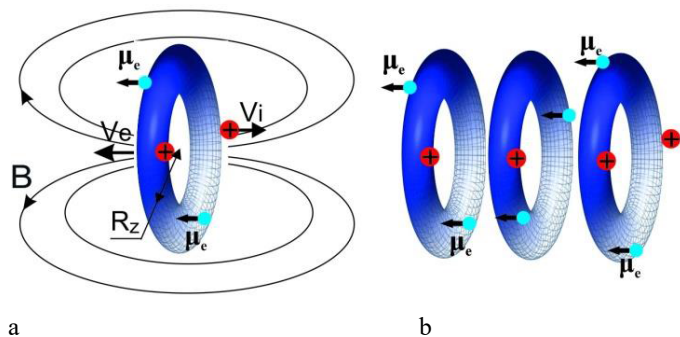


Figure 12: a – orthoboson, b – “capsule”.

The atoms are transformed into transatoms in internal strong, more than 30 T, magnetic fields \mathbf{B} of the “capsules” [11]. Electrons in a transatom are also coupled in pairs to form orthobosons. It happens in the following way. All ℓ -s and j-j bonds in a strong magnetic field \mathbf{B} are broken in all atomic electrons and their orbital moments are “frozen-in” in the field. Electron states with identical orbital ℓ and magnetic moments m_ℓ quantum numbers are split into two levels with antiparallel electron spins $s=\pm 1/2$. The frequency of transitions between these levels $m_s=\pm 1/2$ is the same for all electron pairs $\omega=2 \cdot \mu_e B/\hbar$. Electromagnetic interaction of electrons causes them to oscillate near their orbitals. These oscillations are quantized by introducing a new quantum number n_b . The exchange interaction between two electrons and an asymmetry in their oscillations $n_{1e} = -n_{2e}$ enable the electrons to create an orthoboson with $S=1\hbar$. The orbital magnetic moment μ_i of each electron precesses around the magnetic field \mathbf{B} with a frequency $\omega = \mu_e B/\hbar$ and creates its own internal magnetic field B_i rotating with the same frequency. The internal magnetic fields B_i of two electrons stimulate transitions between the levels $m_s=1/2 \rightarrow m_s=-1/2$. Thus, in a strong magnetic field, the spin-orbit interaction of internal electrons, leads, due to intra-atomic electron magnetic resonance (AEMR), to pairing of two atomic electrons into an orthoboson. Atomic electron orthobosons merge into a Bose-Einstein condensate, in which all electron spins and their magnetic moments are parallel to each other (Figure 13).

Consequently, atoms, in a strong magnetic field, inevitably turn into transatoms.

The magnetic moments of electrons generate ultrastrong magnetic fields inside and around transatoms up to $B_s \sim 10^5-10^{10} \text{ T}$ [9]. The internal ultrastrong magnetic field interacts with the magnetic spin and magnetic orbital moments of nucleons in the nucleus, changes the structure of the nucleus and turns it into a Transnucleus. Nucleons in the transnucleus also form orthobosons with $S = 1\hbar$, but these are already nuclear orthobosons. The transnucleus with the surrounding electron orthoboson Bose-Einstein condensate forms a spin nuclide electron condensate.

External ultrastrong magnetic fields of transatoms attract them to each other. Electronic Bose-Einstein condensates of two transatoms are combined into a common condensate. A double nuclear transmolecule is formed from their transnuclei. Other transnuclei can join it. A multinuclear transmolecule is formed, in which multinuclear reactions take place, including those with electron orthobosons. Thus, nuclear-electronic reactions occur, which products are non-radioactive. These reactions occur due to the resonant interference exchange interaction (RIEX) [12].

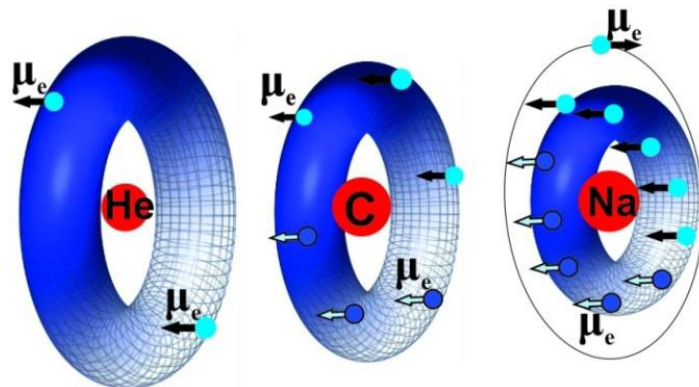


Figure 13: Examples of transatoms: helium, carbon, sodium.

The nature of RIEX interaction is associated with the overlap and interference of the wave functions of objects that have resonant R -states, $\psi_R(R)$. Resonant interference exchange interaction is an exchange interaction between any two or more objects, including between atomic nuclei A, B, C, \dots , which have resonant R -states belonging to a composite system that consists of these objects [6, 12]. The wave functions of the nuclei, $\psi_a(A), \psi_b(B), \psi_c(C) \dots$ interfere with each other in the R -state. The wave functions of the resonant R -states contain all wave functions of the nuclei A, B, C, \dots . Thus, we can say that objects A, B, C are “identical” to each other in the R -state with a generalized similarity coefficient K^2 . It is namely due to the wave functions of R -states that atomic nuclei are simultaneously “in each other” through exchange interactions with each other (Figure 14). R -states are excited on the length of the wave functions of objects A, B, C, \dots . Thus, short-range strong and local weak interactions between nuclei become “long-range” interactions. Strong-weak, electromagnetic and inertial-gravitational interactions are realized between the nuclei simultaneously. RIEX interaction is characterized by the interference of all types of interaction.

Transmutation reactions can be represented as reactions of nucleon and multinucleon transfers between transnuclei with a possible conversion of protons into neutrons and vice versa, as well as reactions of radiationless fusion and fission of transnuclei. Thus, multinuclear, radiationless and low-energy nuclear reactions occur due to the RIEX interaction.

Consequently, atoms, in a strong magnetic field, in weakly excited condensed matter inevitably enter into low-energy nuclear reactions.

Due to exchange forces in weakly excited condensed matter,

ordinary liquid and gaseous media turn into quantum media, and their theoretical and experimental studies will make it possible to control low-energy nuclear reactions, and not just that. Numerous experiments on low-energy transmutation reactions have shown that nuclear reactions occur at low energies in weakly excited condensed matter. The properties of transmutation reactions contradict the properties of conventional nuclear reactions. The discovery of new low energy nuclear reactions and a new resonant interference exchange interaction gives grounds to assert that a necessary and inevitable process of changing the scientific paradigm is currently taking place [6,14]. It is necessary to understand for the transition to a new paradigm that nuclear reactions occur at low energies in condensed matter, in strong magnetic fields (in the reaction volume < 10 eV/atom), and they occur everywhere in the Universe.

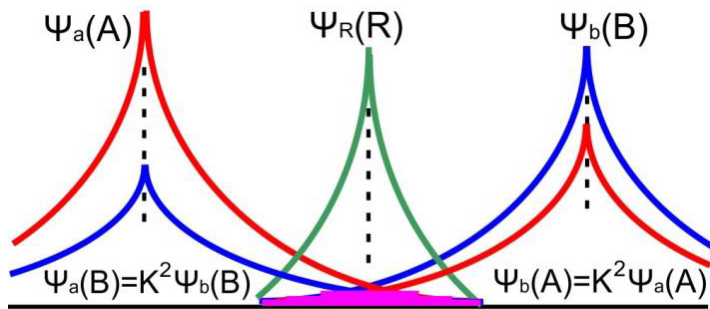


Figure 14: Overlap of wave functions of “identical” objects A and B during the formation of the R-state.

Conclusion

Taking into account the entire set of data obtained with an X-ray microprobe method, it can be argued that in experiment on the irradiation by electrons of the mixture of helium and deuterium under high pressure there is no significant difference in the distribution of chemical elements for the parts of the reaction chamber: the free objects (Figure. 5), the bipartite sleeve (Figure. 7) and the cork-window (Figure 11,12).

The distributions of the synthesized chemical elements in experiment on the irradiation by electrons of the mixture of helium with deuterium (Figure. 15) and in the experiments on the irradiation by gamma-quanta of condensed pure helium (Figure. 16) and pure deuterium (Figure 17) differ little in character from each other. For comparison, Figure. 15 shows the total, averaged over 4 measurements (Tables 1+2+4+5) concentrations of chemical elements for the experiment He+D₂. Figure. 16 shows averaged concentrations of chemical elements determined by 5 measurements for the experiment with pure helium: two measurements were done at the carbon foil and the other three, at the micro particles. Figure 17 shows the averaged concentrations of chemical elements obtained in an experiment on irradiating by gamma-quanta of a chamber with pure deuterium at a pressure of 2.2 kbar [17].

From the above, we can conclude that low-energy nuclear reactions are carried out in high-pressure gases both by their irradiation with gamma quanta and electrons.

Figure 15:

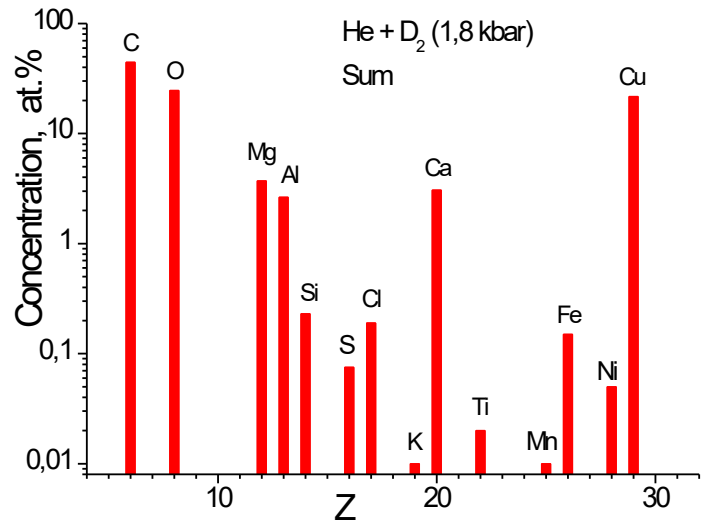


Figure 16:

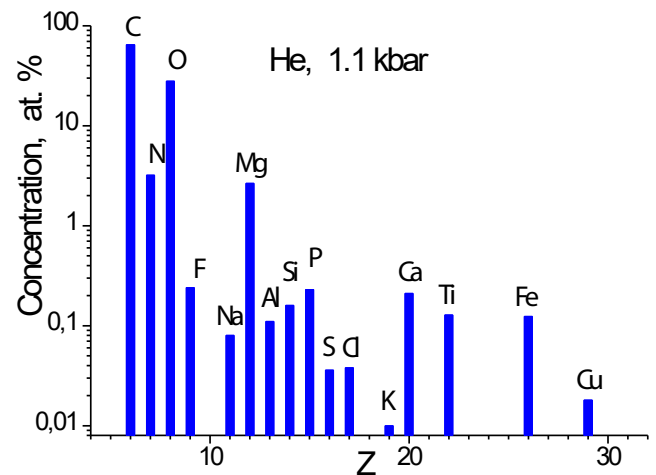
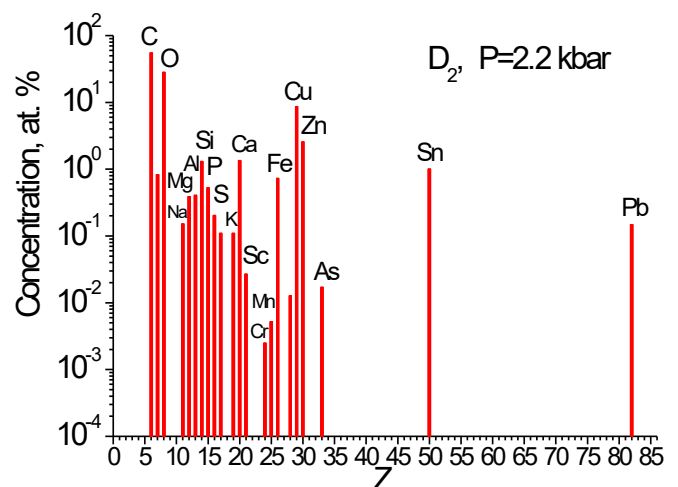


Figure 17:



The theory of low-energy nuclear reactions presented above explains the "main mechanisms" of the effects obtained by the authors. This does not mean that the theoretical side of the problem should not be developed as well as the practical side (physic-chemical processes taking place) in the form of a new nanotechnologies [7,15-18]. Analysis of the value and rate of pressure and temperature changes, assuming that the powers supplied to the inside of the chamber of the system by gamma radiation and by electrons are close to each other may be important. The power supplied in the first case, due to the generation of braking rays in a certain way, is moderately efficient and can be reduced by 20 - 30% than in the second case (with the same energies of maximally accelerated electrons - 10MeV and close electron current intensities 16 and 20 μ A). A faster - by an order of magnitude - increase in temperature and pressure over time, in the second case, may be the basis for drawing a conclusion about the mechanisms of thermal energy supply to the research system, and certainly by way of low-energy nuclear transformations. At the end, photographs with a color distinction of elements on the forehead of the cork of the bipartite bushing, the bipartite bushing and the cork-window were quoted. These images suggest the concentration of elements in the cavities of the surface, which can be seen in particular in the case of the bipartite bushing. In general, a high concentration of such elements as C, O, Mg, (a strong underestimation of the base element Cu) makes the results of the experiment unambiguous. The emergency end of the second experiment did not allow performing an analysis of the composition of the mixture, which would be additional information in the interpretation of phenomena. Of all the cases of transmutation, in the experiments mentioned in the introduction, the way presented by the authors is the most controllable.

Figure 18: The map of the observed elements. Al case illustration may suggest dirt.

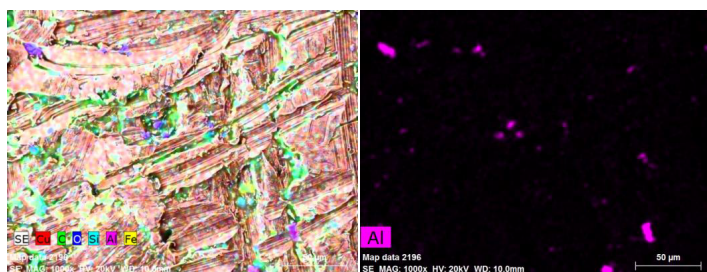


Figure 19: Split sleeve, visible location C and Si in the surface depressions.

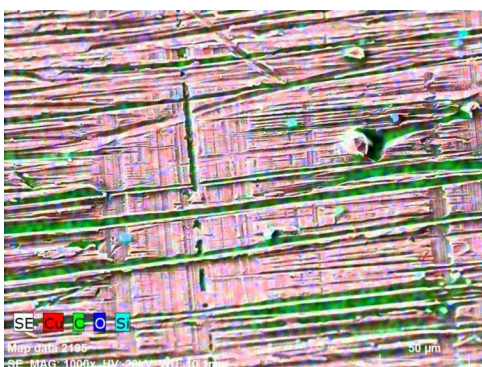
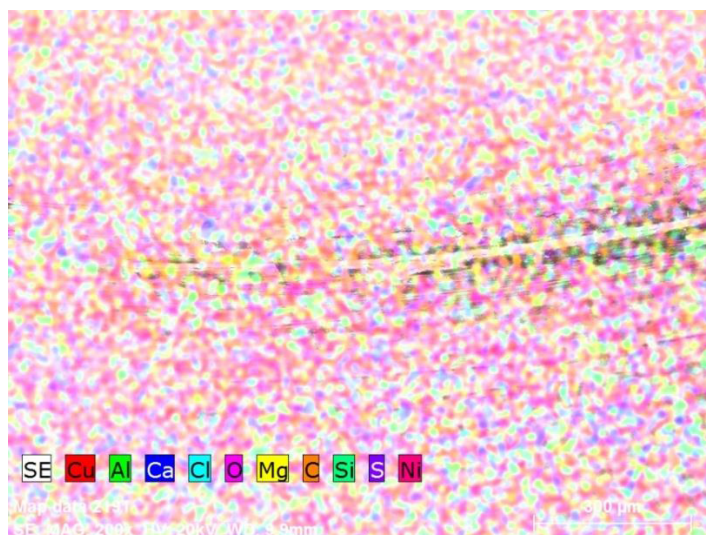


Figure 20: Cork-window - the distribution of elements on a strongly altered side surface.



Are the new elements inside the elements of the apparatus components of a solid, in what places - in the gaps tetrahedral or octahedral, as additional atoms, forming structural errors? Are atoms forming local clusters on the surface of the studied parts, e.g. a two-part sleeve, amorphous or form micro structural objects? These are questions for future researchers. The purity of the copper used was not spectral, but only 99.99% wt. Cu. For the BB2 beryllium bronze used, the situation is less favorable. We have manufacturer data: 1.9% to 2.0% Be, alloy additives Ni + Co (0.2% to 0.4%) and Ti (0.1% to 0.25%). Impurities do not exceed 0.5%. Doubts about the generation of new elements can only concern Ti.

Acknowledgements

The authors of the work would like to thank the Contractor for the photos of the surface of the apparatus parts, for determining the chemical compositions in the near surface (2 μ m) layers, for participating in the interpretation of measuring materials. We would like to thank the staff of the accelerator position in Dubna - as usual - for the highest technical and intellectual help. Thank you to the people who help us in transport the samples, to Directorate - LNR JINR for continuous support of our research (since 2000) - the highest recognition.

References

1. Wiśniewski R. "Synthesis of Chemical Elements and Solid Structures in Atomic-Nuclear Reactions in Dense Gas-Metal Systems Irradiated by γ -Rays". Principles and Applications in Nuclear Engineering. 2018; 3: 49-73.
2. Wiśniewski R, Didyk AYu, Wilczyńska-Kitowska T. Objects Obtained by γ Quanta Irradiation with Threshold Energy of 10 MeV of Pure Gaseous He, under High Pressure, in CuBe2 Apparatus. JPSA. 2015; 5: 268-276.
3. Wiśniewski R, Wilczyńska-Kitows T, Mazerewicz P. Some Physical Properties of Graphite-Like Objects Obtained by γ

- Quanta Irradiation with Threshold Energy of 10 MeV of Pure Gaseous He, under High Pressure, in CuBe₂ Apparatus. JPSA. 2016; 6: 1-11.
4. Wiśniewski R, Didyk AYu. Synthesis of New Structures and Substances in Dense Gases H₂, D₂ and He under Irradiation by Braking 10 MeV γ -rays in Cu_{0.98}Be_{0.02} Pressure Chamber. JPSA. 2016; 6: 13-21.
 5. Didyk AYu, Gulbekian GG, Mishinsky GV, et al. A study of Changes in the Element Composition and Structure of Surfaces under Irradiation of Dense Xenon Gas (270bar) by γ -Rays with Maximum Energy of 10MeV. JPSA. 2016; 6: 18-28.
 6. Mishinsky GV. Towards a new paradigm. RENSIT. 2020; 12: 529-544.
 7. Mishinsky GV. Magnetic fields and high-temperature superconductivity in excited liquids. Unknown particles. RENSIT. 2021; 13: 303-318.
 8. Mishinsky GV. Multinuclear reactions in condensed helium. RENSIT. 2017; 9: 94-105.
 9. <http://www.unconv-science.org/>.
 10. Mishinsky GV. Spin electron condensate. Spin nuclide electron condensate. RENSIT. 2018; 10: 411-424.
 11. Mishinsky GV. Atom in a strong magnetic field. Transformation of atoms to transatoms. RENSIT. 2017; 9: 147-160.
 12. Mishinsky GV. Resonant interference exchange interaction. RENSIT. 2019; 11: 261-278.
 13. Mishinsky GV. Non-Coulomb nuclear reactions of transatoms. Stellar energy and nucleus synthesis. RENSIT. 2018; 10: 35-52.
 14. Mishinsky GV. New paradigm and parametry. RENSIT. 2021; 13: 509-520.
 15. Didyk AYu, Wisniewski R. Synthesis of Microparticles in Molecular Hydrogen at 1kbar Pressure in Nuclear Reaction Induced by Braking γ -Rays of 10MeV Threshold Energy. JINR. 2014; 19: 43.
 16. Wisniewski R, Mishinsky GV, Gulbekian GG, et al. Synthesis of chemical elements and solid-state structures under irradiation by γ -quanta in condensed gases. International Journal of Unconventional Science. 2017; 17-18: 6-15.
 17. Didyk AYu, Wiśniewski R, Mishinsky GV, et al. Synthesis of Solid State Structure and Chemical Elements Under Irradiation by Bremsstrahlung γ -rays with Maximum Energy of 10MeV in Condensed Deuterium at Pressure of 2.2kbar. JINR. 2018; 15: 3.
 18. Didyk AYu, Wiśniewski R, Wilczynka-Kitowska T, et al. Synthesis of chemical elements under irradiation by braking gamma-rays of palladium in condensed gases. RENSIT. 2019; 11: 143-160.

The Historical Appendix



Figure 12: Laboratory for Pressure Investigations ZMJ FCS, DM, NCBJ, Otwock-Świerk, Poland, 2004 - †2014.

Laboratory location: Health Building, second floor, laboratory - room 72, quiet workroom - 68. Largely, the rescued laboratory equipment is now in the *Institute of Biotechnology of the Agricultural and Food Industry* . In 2020, we managed to perform work in the field of Pressure Food Preservation Technologies (in journal: *Progress of Science and Technology of the Agri-Food Industry*).



The view of our portable high-pressure apparatus located in the Mikrotron MT25 electron accelerator system in the Dubna Nuclear Reactions Laboratory JINR. A fragment of the accelerator installation is visible. Completely working equipment of accelerator was in perfect state during our, long-term, cooperation.